OMMYDCLD README

1. Overview

This document describes the OMMYDCLD data product. OMMYDCLD is a Level 2 orbital track product that combines cloud parameters retrieved by the Ozone Mapping Instrument (OMI) on Aura with collocated statistical information for cloud parameters retrieved by the Moderate Resolution Imaging Spectrometer (MODIS) on Aqua. This product is designed to take advantage of the synergy between OMI and MODIS, which both fly on satellites in the NASA A-Train. The A-Train is a constellation of Earth-observing satellites that follow similar orbital tracks and collect near-simultaneous observations as shown in Figure 1. It is envisaged that this product will be used for cloud-clearing, detection of multi-layered clouds, and other applications that may exploit these multi-spectral measurements.

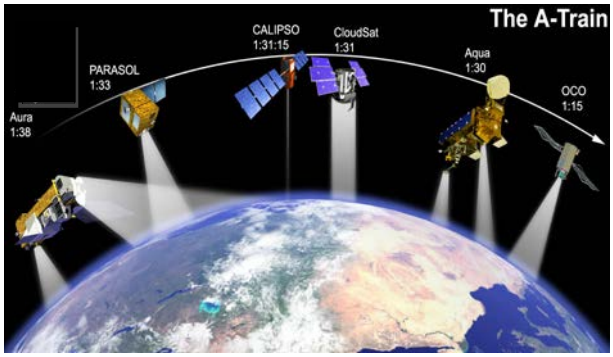

Figure 1. *The A-Train constellation of satellites.*

Since the launch of Aura in 2004, the time lag between the Aura and Aqua has ranged from 15 minutes (2004-2007) to about 8 minutes (2008 -present), as the result of a coordinated effort to bring the two satellites closer together. Figure 2 shows the time lag between Aqua and Aura since January 2005.

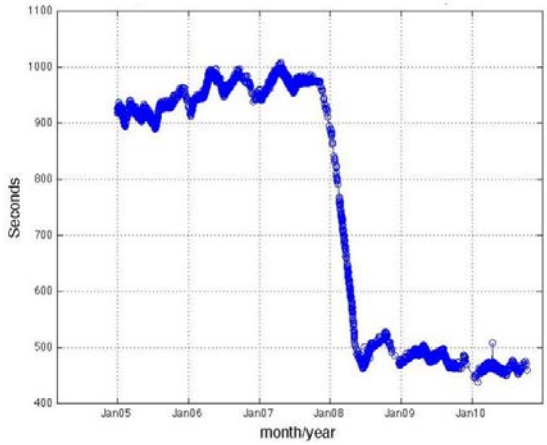

Figure 2. *Plot showing time difference between OMI and MODIS as determined from sequential overpasses of Aeronet sites.*

2. Collocation Algorithm

The algorithm for OMMYDCLD co-locates daytime cloud parameters from MODIS onto the OMI VIS pixel for a given OMI orbit and generates statistical information from the collocated MODIS pixels. For each OMI granule, the orbit start and end times are used to select the corresponding 5-minute MODIS granules for processing. A contiguous list of MODIS granules spanning the full duration of the OMI orbit are selected based on the relative time lag between Aqua and Aura (see Figures 1 and 2). Figure 3 displays a schematic showing the processing of a typical OMI orbit.

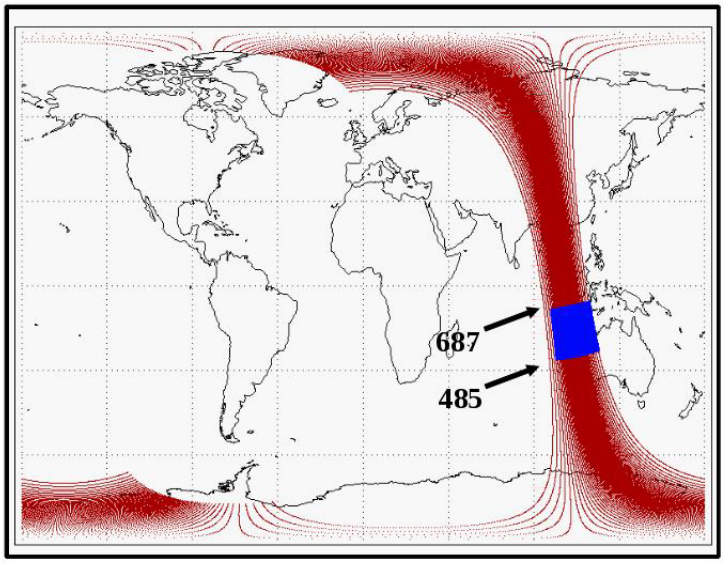

Figure 3. *Schematic showing the processing of OMMYDCLD. The OMI orbit is shown in red and the MODIS granule in blue. The numbers displayed in the figure correspond to the OMI scan line indices enveloping the MODIS orbit.*

As shown in Fig. 3, the beginning and ending times for each MODIS granule are used to constrain the co-location of OMI and MODIS to a narrow range of OMI time indices for the selected orbit. Note that the MODIS granule does not completely cover the OMI swath on the left-side of the orbit (in red). There is no MODIS overlap of OMI rows 1 thru 3.

MODIS 1 and 5 km data fields are co-located onto the OMI pixel using what is known as “crossing number algorithm.” This algorithm can be generally applied to any N-sided polygon. The OMI pixel corner product (OMPIXCOR) is used to define sample space and to define the geo-spatial boundaries of the OMI pixel (see Figure 4). OMIPIXCOR provides corner definitions using two different methods for specifying the VIS OMI pixel corners: 1) 75% power for the OMI field of view (FoV), approximated by a rectangle and 2) tiled. The first method constructs the corners based on 75% TOA retrieved UV/VIS solar energy for the OMI FoV. The cross- track borders for 1) are adjacent but the along-track borders effectively overlap, meaning a MODIS pixel can contribute to the statistics of more than one OMI pixel. The second definition assumes all

four borders are adjacent with no overlap. We use corners generated with method 1) to generate the boundaries for the OMI pixel, which provides a more physical estimate of the OMI FoV.

Defining a sample space constrains the number of MODIS pixels that need to be tested for co-location to a relatively small sample size (~300-600 pixels at the 1 km scale, depending on the OMI across-track position). The sample space shown in Figure 4 is constructed along constant lines of latitude and longitude as determined from minimum and maximum geographical coordinates (latitude, longitude) for the four OMI corners.

The OMI FoV is constructed by connecting the four corners by straight lines (nearly conforms to a rectangle projected onto the Earth's surface). The line crossing method defines a line segment from the center of the MODIS pixel to a test point labeled X in Fig. 4. The point X is arbitrarily defined just outside of the sample space. The line $\overline{AX}$ or ($\overline{BX}$), shown in Fig. 4, is then tested to see how many intersections occur with the line equations constructed for each of the four sides of the OMI pixel ($\overline{S1}$, $\overline{S2}$, $\overline{S3}$, $\overline{S4}$). If the number of line crossings is odd then the MODIS pixel is co-located with OMI, and if the number of crossings is even number, the pixel is excluded from the statistics.

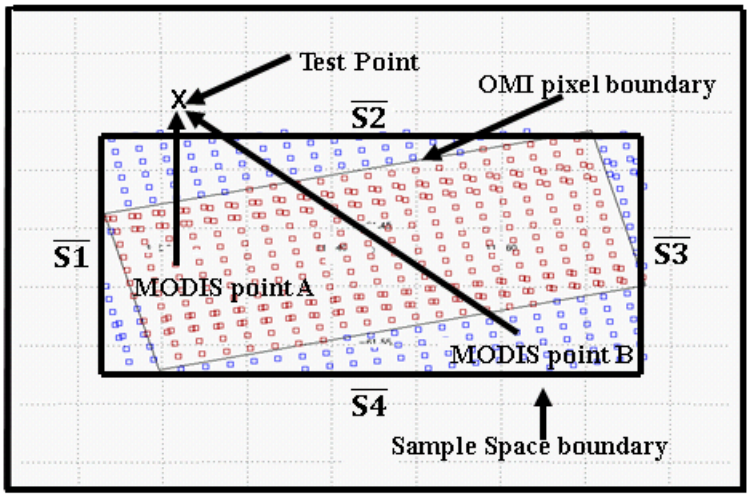

Figure 4. *Illustration of the sample space generated from the OMI pixel corner product. The sample space is defined by the minimum and maximum values of the pixel corner geo-locations. The OMI pixel is embedded in this space. All of the MODIS pixels existing in this space are tested to see if they fall within the boundaries of the OMI pixel. Pixels outline in red were found inside, whereas those in blue were determined to be outside. Two MODIS pixels labeled A and B were selected to illustrate the line crossing technique. Pixel A is found to be inside, whereas Pixel B is found outside of the OMI pixel.*

3. Data Output

The data product OMMYDCLD will provide users with histograms and the first two statistical moments (i.e., mean and standard deviation) for the MODIS 1 km data fields. Only provide the first two statistical moments for the MODIS 5 km data fields.
Some MODIS 1 km cloud fields will be further partitioned into liquid, ice, and combined liquid and ice distributions using the optical cloud phase information (*e.g.*, cloud optical depth, effective particle radius and cloud liquid water path).

4. Data Quality Issues

This section lists some of algorithm issues for users that may affect the accuracy of the information provided.

- The lag time between satellites, though relatively short, can introduce natural variance into the MODIS statistics (relative to the OMI FoVs).
- OMI pixel corners are assumed to be connected by straight lines, not geodesics. This issue can affect the accuracy of the co-location, but it is a reasonable assumption away from the extreme polar-regions. Any additional variance is likely to be very small relative to the variance introduced by the time lag between satellites.
- OMI pixel areas vary in the cross-track direction from 337 (row 30) to 4500 (row 1) km^2, which affects the statistical sample sizes. MODIS data flagged as missing are not included in the statistics, which can reduce nominal sample sizes. Particularly near the edges of cloud structures, MODIS cloud optical properties are not produced and the statistical information from MODIS may not be representative of a given OMI scene. The number of MODIS pixels included in any OMI FoV for a particular product should be checked to ensure consistency.
- The MODIS swath does not overlap OMI rows 1-3. These rows receive fill values for the MODIS fields.

5. Product Description

The OMMYDCLD granule includes a full pole-to-pole daytime OMI orbit (~1643 scans) and provides merged data fields for the region of the OMI swath where OMI and MODIS overlap. The OMI swath for UV-2 and VIS consists of 60 pixels or rows with a nominal area of 13 x 24 km^2 at nadir. The width of the OMI swath along the cross track is 2600 km compared to 2300 km for MODIS, which provides overlapping coverage of OMI rows 4 through 60. The indexing for each granule subsequently matches the OMI VIS indexing for the sunlit portion of the orbit.

MODIS cloud information will provide users with data fields such as cloud-top pressure, cloud optical depth, geometrical cloud fraction, effective particle size, and the thermodynamic phase of the cloud. For a complete list of the data fields, users should refer to the file specification document for a list and descriptions of the MODIS data fields. The product also provides cloud/aerosol optical center pressure, effective cloud

fraction, and reflectivity fields from the two OMI cloud products, OMCLDRR and OMCLDO2, and the Aerosol Index from the OMTO3 product. For an overview of OMI cloud products, please consult *Stammes et al*. (2008). Validation of OMI cloud products is described in *Sneep et al.* (2008), *Vasilkov et al.* (2008), and *Joiner et al.* (2012). Description of the MODIS cloud products derived from thermal, visible, and near-IR band can be found in e.g., *Platnick et al.* (2003), *Menzel et al.* (2008), and at http://modis-atmos.gsfc.nasa.gov/MOD06_L2/. Other OMI ancillary information includes fields related to viewing geometry and other physical aspects of an OMI FoV, such as latitude, longitude, solar zenith angle, satellite zenith angle, relative azimuth angle, ground surface classification (land, ocean, coast, etc.), and the area of the OMI pixel (75% FoV power) as a function of the cross track.

Note that the OMI effective cloud fractions are not the same as the MODIS geometrical cloud fraction and these should not be directly compared. Similarly, the OMI cloud/aerosol optical centroid pressures (OCP) are different from the cloud-top pressure (CTP) provided by MODIS, and again these should not be directly compared. The combination of OMI cloud OCP and MODIS CTP can be used to detect multi-layered clouds as described by *Joiner et al.* (2010).

The OMMYDCLD product is generated in an HDF-EOS5 swath file. For a list of tools that read HDF-EOS5 data files, please visit this link: *http://disc.gsfc.nasa.gov/Aura/tools.shtml*.

Questions related to the OMMYDCLD dataset should be directed to the GES DAAC. Users interested in these parameters, or having other questions regarding the OMMYDCLD dataset are advised to contact Brad fisher (bradford.fisher@ssaihq.com) or Joanna Joiner (Joanna.Joiner@nasa.gov).

Haines, Eric, "Point in Polygon Strategies," Graphics Gems IV, ed. Paul Heckbert, Academic Press, p. 24-46, 1994.

Joiner, J., Vasilkov, A. P., Bhartia, P. K., Wind, G., Platnick, S., and Menzel, W. P. , 2010: Detection of multi-layer and vertically-extended clouds using A-train sensors, *Atmos. Meas. Tech.*, **3**, 233-247. Paper available online.

Joiner, J., Vasilkov, A. P., Gupta, P., Bhartia, P. K., Veefkind, P., Sneep, M., de Haan, J., Polonsky, I., and Spurr, R., 2012: Fast simulators for satellite cloud optical centroid pressure retrievals; evaluation of OMI cloud retrievals, *Atmos. Meas. Tech.*, **5**, 529-545, doi:10.5194/amt-5-529-2012. Paper available online.

Menzel, W. P., Frey, R., Zhang,~H., Wylie, D. P., Moeller, C., Holz, R., Maddux,~B., Baum, B. A., Strabala, K. I., and Gumley, L., 2008: MODIS global cloud-top pressure and amount estimation: algorithm description and results, *J. Appl. Meteorol. Clim.*, **47**, 1175-1198.

Platnick, S., King, M. D., Ackerman, S. A., Menzel, W. P., Baum, B. A., Riedi, J. C., and Frey, R. A., 2003: The MODIS cloud products: algorithms and examples from Terra, *IEEE T. Geosci. Remote*, **41**, 459-473.

Sneep, M., J. F. de Haan, P. Stammes, P. Wang, C. Vanbauce, J. Joiner, A. P. Vasilkov, and P. F. Levelt, 2008: Three-way comparison between OMI and PARASOL cloud pressure products, *J. Geophys. Res.*, **113**, D15S23, doi:10.1029/2007JD008694.

Stammes, P., Sneep, M., de Haan, J. F., Veefkind, J. P., Wang, P., and Levelt, P. F, 2008: Effective cloud fractions from the Ozone Monitoring Instrument: Theoretical framework and validation, *J. Geophys. Res.*, **113**, D16S38, doi:10.1029/2007JD008820.

Vasilkov, A. P., J. Joiner, R. Spurr, P. K. Bhartia, P. F. Levelt, and G. Stephens, 2008: Evaluation of the OMI cloud pressures derived from rotational Raman scattering by comparisons with satellite data and radiative transfer simulations, *J. Geophys. Res.*, **113**, D15S19, doi:10.1029/2007JD008689.